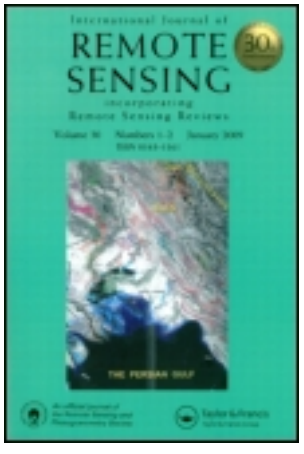
This article was downloaded by: [41.196.240.116]
On: 13 March 2014, At: 15:41
Publisher: Taylor & Francis
Informa Ltd Registered in England and Wales Registered Number: 1072954 Registered office: Mortimer House, 37-41 Mortimer Street, London W1T 3JH, UK



International Journal of Remote Sensing

Publication details, including instructions for authors and subscription information:
http://www.tandfonline.com/loi/tres20

Change detection of coral reef habitat using Landsat-5 TM, Landsat 7 ETM+ and Landsat 8 OLI data in the Red Sea (Hurghada, Egypt)

H. El-Askary[abc], S. H. Abd El-Mawla[de], J. Li[a], M. M. El-Hattab[f] & M. El-Raey[e]

[a] School of Earth and Environmental Sciences, Schmid College of Science and Technology, Chapman University, Orange, CA, USA

[b] Center of Excellence in Earth Systems Modeling and Observation, Chapman University, Orange, CA, USA

[c] Department of Environmental Sciences, Faculty of Science, Alexandria University, Alexandria 21522, Egypt

[d] Department of Environment Protection and Crisis Management, Integrated Simulator Complex, Arab Academy for Science, Technology and Maritime Transport, Alexandria, Egypt

[e] Institute of Graduate Studies and Research, Alexandria University, Alexandria, Egypt

[f] Department of Natural Resources Survey, Institute of Environmental Studies and Research, University of Sadat City (USC), Sadat City, Egypt

Published online: 11 Mar 2014.

To cite this article: H. El-Askary, S. H. Abd El-Mawla, J. Li, M. M. El-Hattab & M. El-Raey (2014) Change detection of coral reef habitat using Landsat-5 TM, Landsat 7 ETM+ and Landsat 8 OLI data in the Red Sea (Hurghada, Egypt), International Journal of Remote Sensing, 35:6, 2327-2346

To link to this article: http://dx.doi.org/10.1080/01431161.2014.894656

PLEASE SCROLL DOWN FOR ARTICLE

Taylor & Francis makes every effort to ensure the accuracy of all the information (the "Content") contained in the publications on our platform. However, Taylor & Francis, our agents, and our licensors make no representations or warranties whatsoever as to the accuracy, completeness, or suitability for any purpose of the Content. Any opinions

and views expressed in this publication are the opinions and views of the authors, and are not the views of or endorsed by Taylor & Francis. The accuracy of the Content should not be relied upon and should be independently verified with primary sources of information. Taylor and Francis shall not be liable for any losses, actions, claims, proceedings, demands, costs, expenses, damages, and other liabilities whatsoever or howsoever caused arising directly or indirectly in connection with, in relation to or arising out of the use of the Content.

This article may be used for research, teaching, and private study purposes. Any substantial or systematic reproduction, redistribution, reselling, loan, sub-licensing, systematic supply, or distribution in any form to anyone is expressly forbidden. Terms & Conditions of access and use can be found at http://www.tandfonline.com/page/terms-and-conditions

Downloaded by [41.196.240.116] at 15:41 13 March 2014

International Journal of Remote Sensing, 2014
Vol. 35, No. 6, 2327–2346, http://dx.doi.org/10.1080/01431161.2014.894656

Taylor & Francis
Taylor & Francis Group

Change detection of coral reef habitat using Landsat-5 TM, Landsat 7 ETM+ and Landsat 8 OLI data in the Red Sea (Hurghada, Egypt)

H. El-Askary[a,b,c]*, S. H. Abd El-Mawla[d,e], J. Li[a], M. M. El-Hattab[f], and M. El-Raey[e]

[a]*School of Earth and Environmental Sciences, Schmid College of Science and Technology, Chapman University, Orange, CA, USA;* [b]*Center of Excellence in Earth Systems Modeling and Observation, Chapman University, Orange, CA, USA;* [c]*Department of Environmental Sciences, Faculty of Science, Alexandria University, Alexandria 21522, Egypt;* [d]*Department of Environment Protection and Crisis Management, Integrated Simulator Complex, Arab Academy for Science, Technology and Maritime Transport, Alexandria, Egypt;* [e]*Institute of Graduate Studies and Research, Alexandria University, Alexandria, Egypt;* [f]*Department of Natural Resources Survey, Institute of Environmental Studies and Research, University of Sadat City (USC), Sadat City, Egypt*

(*Received 31 May 2013; accepted 4 November 2013*)

Owing to continuing touristic developments in Hurghada, Egypt, several coral reef habitats have suffered major deterioration between 1987 and 2013, either by being bleached or totally lost. Such alterations in coral reef habitats have been well observed in their varying distributions using change detection analysis applied to a Landsat 5 image representing 1987, a Landsat 7 image representing 2000, and a Landsat 8 image representing 2013. Different processing techniques were carried out over the three images, including but not limited to rectification, masking, water column correction, classification, and change detection statistics. The supervised classifications performed over the three scenes show five significant marine-related classes, namely coral, sand subtidal, sand intertidal, macro-algae, and seagrass, in different degrees of abundance. The change detection statistics obtained from the classified scenes of 1987 and 2000 reveal a significant increase in the macro-algae and seagrass classes (93 and 47%, respectively). However, major decreases of 41, 40, and 37% are observed in the sand intertidal, coral, and sand subtidal classes, respectively. On the other hand, the change detection statistics obtained from the classified scenes of 2000 and 2013 revealed increases in sand subtidal and macro-algae classes by 14 and 19%, respectively, while major decreases of 49%, 46% and 74% are observed in the sand intertidal, coral, and seagrass classes, respectively.

Downloaded by [41.196.240.116] at 15:41 13 March 2014

1. Introduction

Coral reefs suffer major deterioration and degradation due to natural and man-made impacts worldwide. Worst-case estimates of reef degradation predict that almost half of the world's reefs may be irrevocably lost in the next 30 years (Wilkinson 2000). Hence, close monitoring is needed to save such vital components of our environment. Traditionally, reef health has been estimated using expensive and tedious underwater surveying techniques that, by definition, cannot cover large areas (PCRF 2002). Remote-sensing technology serves as an important means of monitoring and surveying large and remote areas of coral reefs distributed worldwide in a cost- and time-effective manner (El-Raey et al. 1996; Kutser, Dekker, and Skirving 2003). However, it is not a simple task because of the varying optical properties and spatial distributions of the reef

*Corresponding author. Email:elaskary@chapman.edu

© 2014 Taylor & Francis

Downloaded by [41.196.240.116] at 15:41 13 March 2014

communities and their subsequent assessment complexity. The most common sensors suitable for coral reef identification and classification are SPOT High-Resolution Visible (HRV), Landsat Multispectral Scanner (MSS), Thematic Mapper (TM), Enhanced Thematic Mapper Plus (ETM+), Operational Land Imager (OLI), IKONOS, Advanced Airborne Hyperspectral Imaging System (AAHIS), and Airborne Visible/Infrared Imaging Spectrometer (AVIRIS) (Atkinson et al. 2001; Hochberg and Atkinson 2003). The classification accuracies obtained for the AVIRIS, AAHIS, IKONOS, Landsat ETM+ , and SPOT HRV sensors are reported as 98%, 98%, 64%, 58%, and 50%, respectively (Hochberg and Atkinson 2003). A natural reef environment is an arrangement of coral, algae, sand, and other biotic and abiotic components that are spatially heterogeneous on scales of millimetres to tens of metres (Stoddart 1969). It has been found that coral reefs generally exhibit a unique geomorphologic zonation pattern as a result of the interaction between reef developmental processes and the oceanic physical environment (Stoddart 1969). Typical zones include the fore reef, reef crest, reef flat, back reef, and lagoon with pinnacles (Vanderstraete, Goossens, and Ghabour 2004). Reef zone degradation is observed when mass coral mortality occurs followed by a formation of an algal mat growing on the coral skeletons (Done 1992). Such phase shifts that change community structure may occur slowly or precipitously, depending on how favourable the conditions are for algal growth (Done 1992). Optical sensing methods typically penetrate clear waters to approximately 15–30 m depending on water quality. Yet, light penetration is wavelength dependent, being greater over the blue spectrum (400 nm) than, for instance, the red spectrum (600 nm) (Mumby et al. 2004). Reflectance of reef communities (coral, algae, and sand) shows an increase in the visible range from 400 to 700 nm with a degree of local minimum near 675 nm due to chlorophyll absorption (Hochberg and Atkinson 2003). However, sand is much brighter than coral and algae, which have nearly equivalent spectra except for slight differences over the curvature covering the range 500–625 nm (Hochberg and Atkinson 2003). Therefore, it is evident that spectral resolution is more important than spatial resolution for discriminating between reef communities (Hochberg and Atkinson 2003; Mumby et al. 1997). Therefore, several well-placed, narrow (10 nm) spectral bands are necessary to detect subtle differences in reflectance between some reef communities (e.g. seagrass vs. algal beds, coral vs. algae, brown algae vs. green algae) (Hochberg and Atkinson 2003). However, ecosystem complexity and the degree of detail addressed in a research question play a pivotal role in deciding resolution accuracy both spatially and spectrally. For instance, higher spectral resolution is needed when analysing changes in just the main groups of organisms (i.e. coral vs. alga), but higher spatial and spectral resolutions are needed when measuring changes within the coral species communities – which is not the scope of this paper.

Coral reefs in Egypt represent an attractive factor for tourism and national income. Moreover, they provide a primary indicator for environmental balance and reflect different environmental stressors. Limited research has been carried out for the Hurghada region, giving the baseline information needed to assess and manage coral reef systems. In the current research we used Landsat TM and ETM+ sensors, which showed potential as important tools for researchers to map coral reefs (Ahmad and Neil 1994; Biña et al. 1978; Smith, Rogers, and Reed 1975). A Landsat 7 ETM+ data set was used to classify and identify the different bottom types occurring in the reefs offshore of Hurghada (Vanderstraete, Goossens, and Ghabour 2004). Moufaddal (2005) performed multi-date change analysis on a Landsat 5 TM image from 1984 and a Landsat 7 ETM+ image from 2000 to identify the impacts of human activities on coastal habitats (e.g. coral reef and seagrass) over Hurghada. Furthermore, Vanderstraete, Goossens, and Ghabour (2006)

examined changes in coral reef composition, including coral, macro-algae, seagrass, and sand, using a Landsat 5 TM image from 1987 and a Landsat 7 ETM+ image from 2000 over the same area. However, these analyses did not provide change detection statistics to quantify coral reef changes in Hurghada. This work therefore aims to investigate and shed light on coral reef health in a trial to develop a more exhaustive foundation for present and future coral reef scenarios, by highlighting possible causes or changes that have degraded coral reefs for the last two decades as shown by our change detection analysis of scenes from 1987, 2000, and 2013. The more recent data used in this analysis were obtained by incorporating observations from the newly launched Landsat 8, which helped us overcome problems associated with data from Landsat 7 in regard to our 2000 image.

2. Study area

The Red Sea supports some of the world's most significant coral reefs and other related marine resources due to its globally distinct oceanographic and geologic evolution. It is completely surrounded by deserts, and hence has almost no water input from rivers. Therefore, the region exhibits very stable physical characteristics such as salinity, temperature, and water quality (Edwards 1987). However, since the 1960s, human interference with the natural environment has steadily increased, leading to negative impacts on the health and status of these coral reefs (Pilcher and Alsuhaibany 2000). The situation becomes especially worrisome in the northwestern part of the Red Sea, where major threats are dominant. These threats include the booming tourism industry and urban coastal development projects, mainly established for tourist accommodation and in support of the Egyptian relocation policy (Wilson 1998). Key habitats and animal life that require attention are coral reefs, seagrass beds and mangroves, sponges, cnidarians, molluscs, echinoderms, worms, tunicates, reef fish, sea turtles, sea birds, and marine mammals. Our analysis considered the coral reefs near Hurghada, Egypt (27° 14′ N, 33° 54′ E), situated in the northern part of the Red Sea (Figure 1). Previous research has targeted the same region, where field measurements were taken into consideration (Vanderstraete, Goossens, and Ghabour 2004). This area covers about 150,000 ha and has an altitude ranging from 0 m to mountains at 300 m above sea level. Hurghada is characterized by a warm temperature throughout the year and a dry desert climate with a steady breeze. It suffers from very hot summers, with temperatures between 26 and 34°C; however, during winter time, the temperature falls to 20–25°C and water temperature reaches 20–22°C. Hurghada exhibits a wide variety of coral reef types with a structural complexity unmatched on earth, and their diversity is greater than anywhere else in the Indian Ocean (PERSGA 2004).

3. Data used

Three images, from Landsat-5 TM, Landsat-7 ETM+, and Landsat-8 OLI with 30 m spatial resolution were used in the change detection analysis, over a 26-year period. The 1987 image, which represents TM, was acquired on 14 August 1987; the 2000 image, which represents ETM+, was acquired on 10 September 2000; and the 2013 image, which represents OLI, was acquired on 20 July 2013. All scenes were obtained from path/row number 174/41, are cloud-free, and were projected to UTM 36 zone at reference datum WGS 84. The image analysis and processing for all images were carried out using ENVI and ERDAS IMAGINE.

Downloaded by [41.196.240.116] at 15:41 13 March 2014

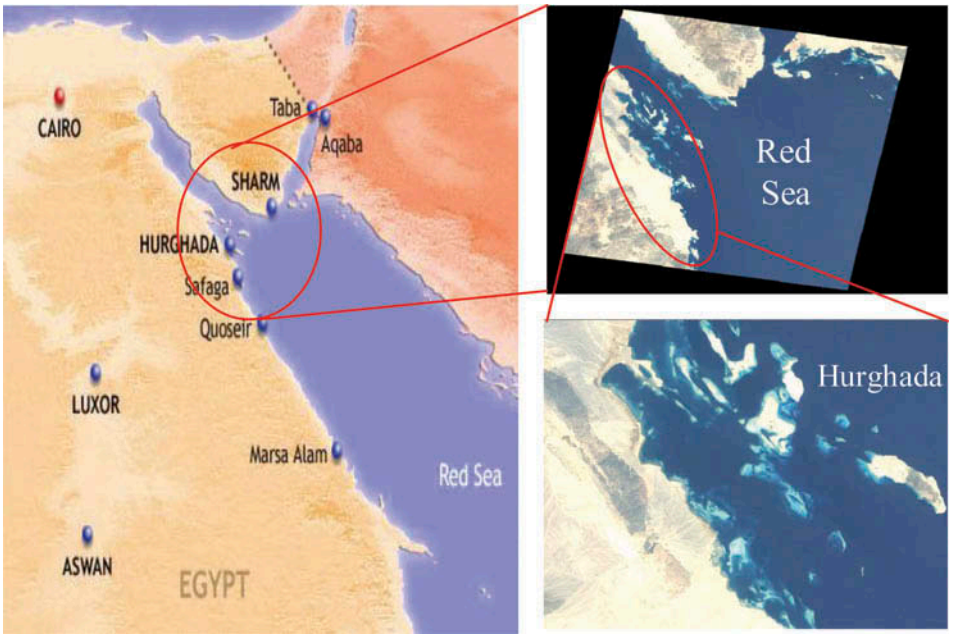


Figure 1. Base map showing the location of Hurghada.

4. Methodology

4.1. Image preprocessing

Three images were preprocessed prior to the classification and change detection analysis. The visible bands (0.4–0.7 μm) were used for the analysis due to lower water column absorption at these wavelengths. Moreover, these bands have spectral ranges that help to identify the water–land interface. Image rectification was first applied to the 1987 and 2013 scenes using the 2000 scene, with the UTM 36 zone projected as a base image. Around 15 ground control points (GCPs) were selected interactively from both sources and reference images. The root mean square (RMS) error was minimized to 0.4 pixels while the rotation, scaling, and translation (RST) method was used with nearest-neighbour resampling. The water body was then separated from the coral reef ecosystem using masks. This was carried out because the water body and coral reef have similar spectral reflectance, which may lead to misclassification in water/coral areas. Moreover, no significant reflection of seabed is noticed in deep water, as discussed by Vanderstraete, Goossens, and Ghabour (2004). The different stages used through the masking process are shown in Figure 2 and are summarized as follows.

- Subsetting: An area of interest (AOI) window is highlighted over the Hurghada region and separated from three scenes.
- Classification: An unsupervised classification was performed to the subset image to create a thematic raster layer using an ISODATA clustering method in which the minimum spectral distance formula is used for 150 iterations with a convergence threshold accuracy of 0.99 to form clusters.
- Recoding: Each value generated from the unsupervised classification is assigned to a symbol or code to discriminate pixels related to sea (code W), coral (code C), or

Downloaded by [41.196.240.116] at 15:41 13 March 2014

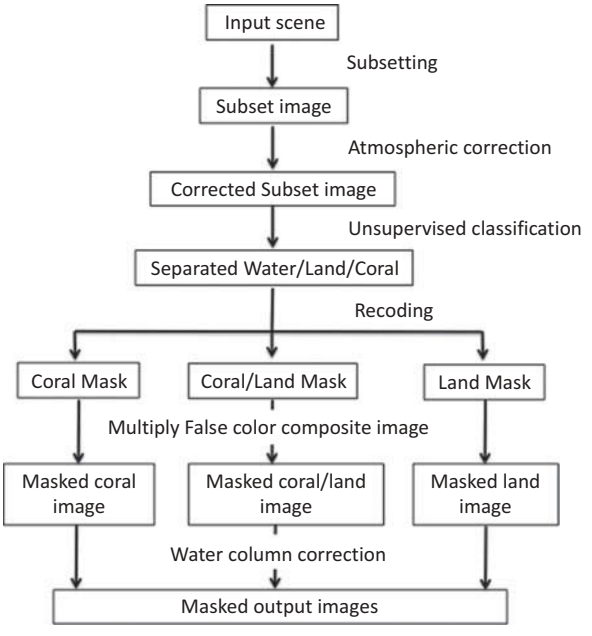


Figure 2. Masking, atmospheric, and water column correction processes for original satellite images for 1987, 2000, and 2013.

land (code L). Masked coral/land scenes were obtained by assigning C and L to 1 and W to 0. Moreover, masked coral scenes were obtained by assigning C to 1 and L and W to 0.

- Multiplying: The final step, shown in Figure 3, aims to process a function that uses codes with a value of 1, and multiplying this by the subsetted false-colour composite image to generate the final masked image Water column correction is then applied to these final masked images.

4.2. *Water column correction*

It is evident that depth-invariant processing of digital spectral data improves the accuracy of marine habitat mapping using multispectral classification; hence, water column correction is most appropriate for imagery with several water-penetrating spectral bands (e.g. Landsat TM) (Lyzenga 1981; Maritorena 1996). Therefore, depth-invariant processing was performed in this study to assess whether any significant changes in habitats had occurred during the 26 year period. Critical to such assessment would be a clear measure of how accurate the classifications might be, based on end member selected data. This would demonstrate the level of confusion (misclassification) between the macro-algae, seagrass, and coral classes, which are spectrally similar. Also, this would provide information on the differences due to the inherent limitations of the imagery. When light penetrates water its intensity decreases exponentially with increasing depth. This process is known as attenuation, which is wavelength dependent, and exerts a profound effect on remotely sensed data of aquatic environments (Green et al. 2000). In the visible region, the red part of the spectrum attenuates more rapidly than the shorter-wavelength blue part.

Downloaded by [41.196.240.116] at 15:41 13 March 2014

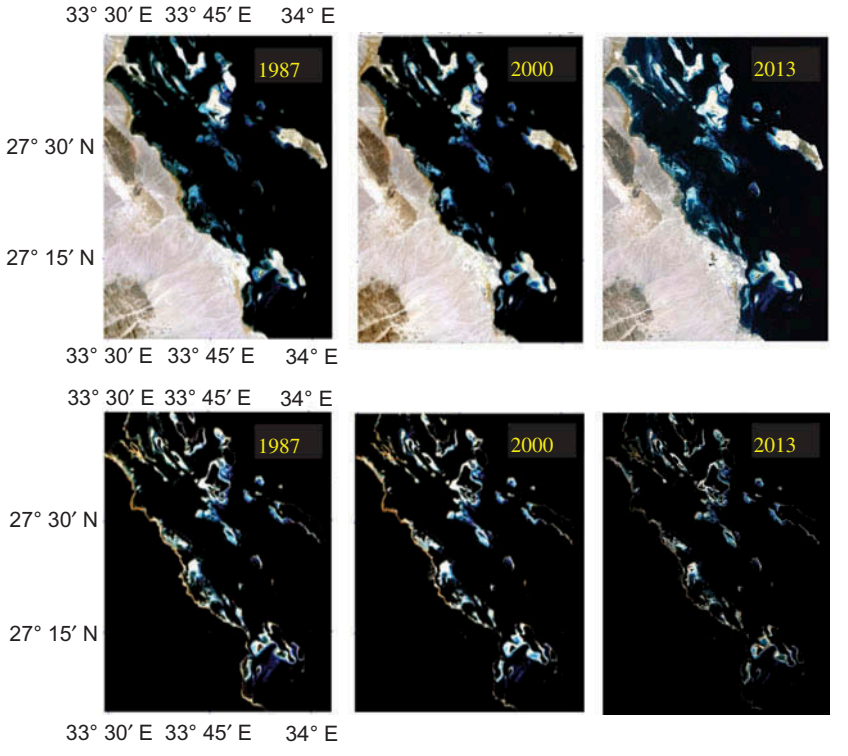


Figure 3. Images from masking process for 1987, 2000, and 2013, Masked coral/land (top), masked coral (bottom) in each pair.

As depth increases, the separability of habitat spectra declines (Green et al. 2000). The spectral radiances recorded by a sensor are therefore dependent on both the reflectance of the substrata and depth. These two influences on the signal can create considerable confusion when attempting to use visual inspection or multispectral classification to map habitats. Since most marine habitat-mapping exercises are only concerned with mapping benthic features, it is useful to remove the confounding influence of variable water depth. This method is applicable to clear waters such as those in coral reef environments. The irradiance diffuse attenuation coefficient (hereafter referred to as k) describes the severity of light attenuation in water for that spectral band (Green et al. 2000). It is related to radiance and depth by

$$L_i = L_{si} + a_i \cdot r_i \cdot e^{-2k_i z}, \tag{1}$$

where, L_i is the radiance in band i, L_{si} is the mean radiance of deep water in band i, a_i is a constant, r_i is the bottom reflectance, k_i is the attenuation coefficient of band i, and z is the depth. By rearranging the above equation using a natural logarithm to generate an image of bottom type for band i, we obtain

$$\ln(L_i - L_{si}) = \ln(a_i \cdot r_i) - 2k_i z. \tag{1a}$$

By applying the same concept for band j, we obtain

Downloaded by [41.196.240.116] at 15:41 13 March 2014

$$\ln(L_j - L_{sj}) = \ln(a_j \cdot r_j) - 2k_j z. \quad (1b)$$

By eliminating z between Equations (1a) and (1b), we obtain

$$\ln(L_i - L_{si}) - \left[\left(\frac{k_i}{k_j}\right) \cdot \ln(L_j - L_{sj})\right] = \ln(a_i.r_i) - (k_i/k_j)\ln(a_j.r_j). \quad (2)$$

By looking at the quantity on the right-hand side Equation (2), we find that k_i and k_j are unknown but fixed constants, and we will discuss how their ratio is determined later in this section. On the other hand, the two constants a_i and a_j represent (intensity of sunlight in wavelength range of band i and j, respectively) × (downwards transmission coefficient of this light at the surface of the water) × (upwards transmission coefficient of this light at the surface of the water). Hence, for any given day/image, the intensity of sunlight in these bands is the same over the entire scene and then the expression on the right-hand side of Equation (2) will depend only on r_i and r_j, representing the bottom reflectivity of the two bands i and j for the pixel in question.

Our goal is to generate an image of reflectance, r_i, representing the bottom type, which theoretically can be done if we rearrange Equation (1a). Yet, this approach is not feasible because there are too many unknown quantities for each band, namely three variables in the case of band i (a_i,k_i,z) (i.e. the value of the constant, a_i, mentioned above, the attenuation coefficient, k_i, for band i, and the depth of water at each pixel). The method of Lyzenga (1978, 1981) does not require the actual calculation of these parameters and does not estimate k for each band, but uses the ratio of attenuation coefficients between the pair of bands, k_i/k_j, where k_j is the attenuation coefficient of band j.

This ratio given in Equation (3), following Lyzenga (1981), can be determined from the data *per se* and obviates the need to know a_i and z using the 'depth-invariant bottom index' approach. The physical significance of this approach is that each pixel value for different bottom types is converted to an index of that specific bottom type, which is totally independent of depth. Therefore, pixels from similar habitats will have similar depth-invariant indices corresponding to that specific habitat. This means that if we consider the whole scene and choose only those pixels for which the bottom reflectivity is the same (e.g. coral or any other class, $r_i = r_j$), then all these pixels will have the same value as the depth-invariant index. This leads to the expression on the left-hand side of Equation (2) being known as the depth-invariant index, which is shown in Equation (5).

The depth-invariant bottom index calculation starts by selecting two bands for the same bottom type and producing a bi-plot of their log transformed radiances at varying depths to determine the attenuation coefficient. By doing that, we have linearized the depth effect on the measured radiances of that substratum, and therefore the pixel values for each band will vary linearly according to their depth only. The slope of the bi-plot represents the relative amounts of attenuation in each band. To determine the mean deep water radiance, an area is selected in the data set that represents deep water (i.e. >40 m) (Green et al. 2000). As suggested by Armstrong (1993), two standard deviations are subtracted from the mean in order to account for possible sensor noise. Areas of sand are good because they are fairly recognizable to an interpreter without much field experience (Green et al. 2000). We avoid areas of shallow water (<1 m) in both bands because of little variation in short wavelengths, and thus the resulting bi-plot will have a gradient close to zero and cannot be used to determine the ratio of attenuation coefficients (Green et al.

Downloaded by [41.196.240.116] at 15:41 13 March 2014

2000). In this paper, Equations (3) and (4) shown below are Equations (4) and (5) of Lyzenga (1981):

$$k_i/k_j = a + \sqrt{(a^2 + 1)}, \tag{3}$$

where

$$a = \frac{\sigma_{ii} - \sigma_{jj}}{2\sigma_{ij}}, \tag{4}$$

σ_{ii} is the variance of band i, and σ_{ij} is the covariance between bands i and j.

Since the attenuation result depends on which band is chosen as the dependent variable, the gradient of the line is not calculated using conventional least squares regression analysis. Therefore, rather than calculating the mean square deviation from the regression line in the direction of the dependent variable, the regression line is placed where the mean square deviation (measured perpendicular to the line) is minimized. Then, following Lyzenga (1978, 1981), we calculate the depth-invariant index following the simple equation of a straight line, $y = p + q.x$, where p is the y-intercept and q is the gradient of the regression of y on x. The equation then can be rearranged to give the y-intercept $p = y - q.x$. This is applied here on the bi-plot of the log transformed radiances of two bands for the same bottom type at varying depths, with a slope representing the attenuation coefficient to calculate the depth-invariant index given in Equation 5:

$$\text{depth-invariant index}_{ij} = \ln(L_i - L_{si}) - \left[\left(\frac{k_i}{k_j}\right) \cdot \ln(L_j - L_{sj})\right]. \tag{5}$$

According to the method of Lyzenga, another minor modification was performed, this being the rescaling of values to the axis orthogonal to the bi-plot slope or, in other words, doing an additional orthogonal rotation to align the y-axis along the k_i/k_j gradient. However, this refinement does not alter the functionality of the process (Edwards 1999; Green et al. 2000; Vanderstraete, Goossens, and Ghabour 2004). The present study resulted in three depth-invariant bottom indices – for 1987, 2000, and 2013. Areas of significant change were then highlighted by performing image differencing for each pair of depth-invariant bottom indices for these three years. The resulting difference layers from the three depth-invariant bottom indices produced a binary map highlighting areas of change. This step is quite important in our analysis since we used our training samples for classification purposes from areas exhibiting no change in those binary maps.

Prior to implementation, it is suggested that masking out of land, clouds, and deep water be performed (Edwards 1999; Maritorena 1996; Matsunaga, Hoyano, and Mizukami 2001) by setting all pixels to zero. The depth-invariant algorithm is implemented in image-processing software once the ratios of attenuation coefficients have been calculated for band pairs. Some values of depth-invariant bottom indices are negative, so an offset is incorporated to convert all data to positive values (Green et al. 2000).

4.3. *Classification*

Supervised and unsupervised classifications were performed on masked scenes to identify significant patterns in the images. Unsupervised k-means classification was performed on

Downloaded by [41.196.240.116] at 15:41 13 March 2014

the masked coral images, setting 10 classes defined by the clustering procedure at 5% threshold with the maximum number of iterations capable of separating the 10 classes. Supervised classification was also performed on the masked coral/land and masked coral images, where pixels are grouped into classes that correspond to user-defined training classes, as explained above in 'Section 4.2'. Regions of interest (ROIs) were selected to represent reef ecosystem areas for five marine classes; coral, sand subtidal, sand intertidal, macro-algae, and seagrass. A numerical interpretation key, used to compare examining training samples interpreted from satellite images with representative sample sites collected from the field, was not available. Therefore, field measurements and the satellite image used to classify the Shaab El- Erg sub-area in Hurghada, as performed by Vanderstraete, Goossens, and Ghabour (2004), were used as our reference. Vanderstraete, Goossens, and Ghabour (2004) found that the spatial resolution used is too coarse to map reefs in detail due to spectral mixing in one pixel. Hence, the maximum likelihood classifier was adopted in our study. The advantages of the maximum likelihood classifier are that it employs covariance information and is sensitive to different degrees of variance in the spectral classes (Purkis and Pasterkamp 2004). Classification was followed by thresholding, using a probability image file to screen out misclassified pixels.

4.4. *Change detection*

Change detection analysis is used to identify, describe, and quantify differences between images of the same scene at different times or under different conditions (Lillesand and Kiefer 2000). In this study, the post-classification comparison change detection method was applied to compare the 1987 and 2000 supervised classification maps, as well as the 2000 and 2013 supervised classification maps. Change detection statistics, which tabulate the extent of area experiencing various types of change, were determined for the 1987 and 2000 supervised classification maps, as well as the 2000 and 2013 supervised classification maps.

5. Results and discussion

5.1. *Unsupervised and supervised classification*

The unsupervised *k*-means clustering classification method produced spectral classes based on the natural groupings of the image values without definitive class names. The resulting unsupervised classified images showed different classes according to the class number assigned, change threshold value, and numbers of iterations applied over the masked coral images for 1987, 2000, and 2013, which resulted in different colours in this natural clustering process for each class (see Figure 4). The mis-differentiation between classes is due to the high spectral similarity among the coral subclasses that leads to difficulties in using the unsupervised classification as a tool for identification of different classes. The results of the unsupervised classification shown here did not shed light on applying *k*-means clustering to the masked coral/land image. This is because two spectral extremes are present – coral and land – and hence the clustering method will discriminate only major different coral *versus* land subclasses. This might also result in losing some of the classes belonging to either corals or land because of the strong spectral similarities within each major class (coral vs. land in our case). *k*-means provided us with a degree of knowledge on the possible marine subclasses and highlighted their variability over time, yet with no association to what class types we were observing. Hence supervised

Downloaded by [41.196.240.116] at 15:41 13 March 2014

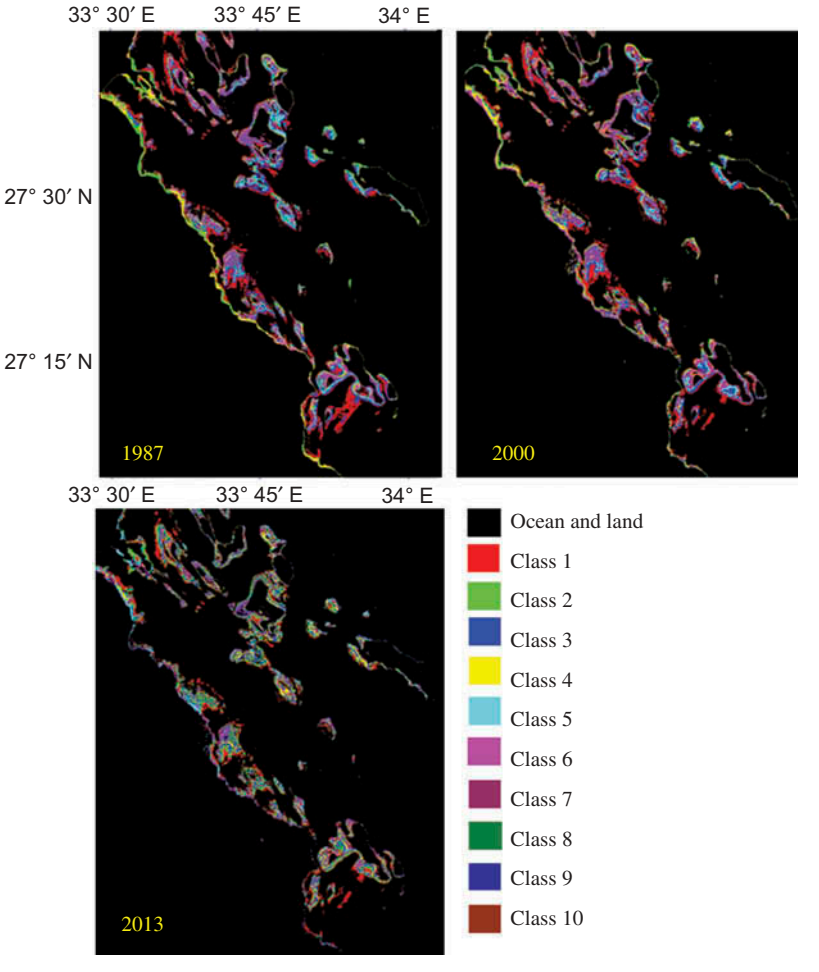


Figure 4. Unsupervised classification results for coral images from 1987, 2000, and 2013.

Downloaded by [41.196.240.116] at 15:41 13 March 2014

classification was performed by creating our own training data set obtained from the Shaab El-Erg sub-area, following Vanderstraete, Goossens, and Ghabour (2004).

Supervised classification results revealed different distribution patterns for the 1987, 2000, and 2013 images (Figure 5). The unclassified pixels, including the masked water or land regions together with others within the marine ecosystem, were assigned to the 'ocean and land' class. Five classes were obtained in coral masked images, yet with different numbers of pixels for each class. Table 1 shows the classification accuracy over time reflected by the lower standard deviation values between the original and classified images for each band in the coral scenes, for the 1987, 2000, and 2013 images. The standard deviation is calculated from the DN of all pixels belonging to one class, which is used to determine the accuracy of classification. The classes obtained appeared at different percentages over spatial and temporal domains. For instance, the coral class is mainly located near shores and around islands in the Red Sea (i.e. mangrove islands). Moreover, sand-related classes are dominant in the 1987 image while macro-algae are dominant in the 2000 and 2013 images. Such variability is discussed in the section on change detection

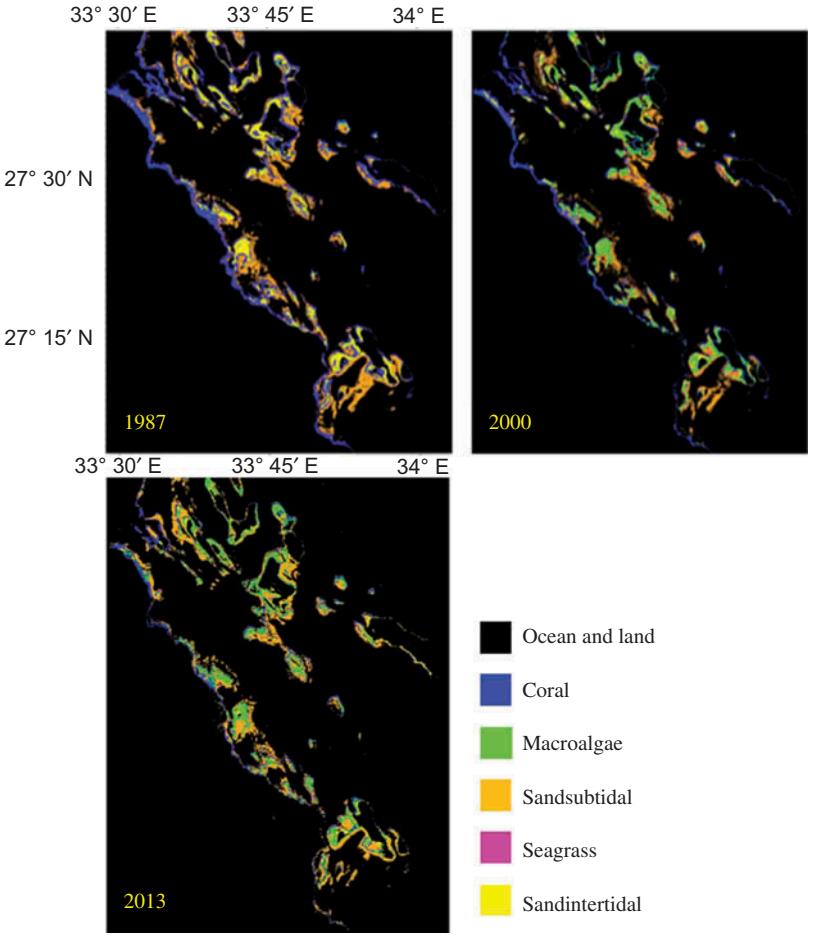


Figure 5. Supervised classification results for coral images from 1987, 2000, and 2013.

Downloaded by [41.196.240.116] at 15:41 13 March 2014

results. For a better quantitative assessment, the output of the thresholding was produced to determine the accuracy for the classified image using the minimum distance classifier. Misclassified pixels appear as black points and were very dominant over the land region, which is outside the scope of this work and is why the coral/land mask image was not used. Few misclassified pixels appeared over the masked sea area, yet the overall assessment agrees with results from previous literature in addition to the new analysis performed in 2013. Marine classes were compared with the Shaab El-Erg classification performed by Vanderstraete, Goossens, and Ghabour (2004) (Figure 6).

5.2. *Change detection analysis*

Figure 7 shows the thematic map representing class changes over the two decades. The resulting map image of difference is colour coded to indicate the magnitude of change between the first and last images (i.e. 2000 and 2013). This analysis focuses primarily on the initial status supervised classification changes (i.e. for each initial status class, the analysis identifies the classes into which those pixels changed in the final status image).

Table 1. Comparison of standard deviation measurements of the original and supervised classification obtained from coral ecosystem images for 1987, 2000, and 2013 scenes.

	Coral	Sand subtidal	Sand intertidal	Macro-algae	Seagrass
			Coral 1987		
Band 1	1.401	1.510	1.603	0.769	0.728
Band 2	0.923	0.758	0.913	0.326	0.327
Band 3	1.160	0.226	1.338	1.008	0.556
Band 4	0.169	0.119	0.231	0.168	0.211
Band 5	0.215	0.155	0.287	0.257	0.281
Band 6	0.134	0.107	0.163	0.143	0.168
			Coral 2000		
Band 1	0.600	0.758	0.526	0.776	0.573
Band 2	0.616	0.904	0.467	0.949	0.150
Band 3	0.689	0.345	0.996	1.567	0.857
Band 4	0.304	0.129	0.395	0.461	0.179
Band 5	0.224	0.143	0.185	0.249	0.121
Band 6	0.188	0.140	0.168	0.195	0.147
			Coral 2013		
Band 2	0.263	0.340	0.549	0.463	0.260
Band 3	0.344	0.424	0.812	0.658	0.413
Band 4	0.504	0.168	1.172	0.940	0.364
Band 5	0.357	0.060	2.037	0.369	0.082
Band 6	0.065	0.044	0.409	0.050	0.060
Band 7	0.045	0.034	0.216	0.038	0.049

Downloaded by [41.196.240.116] at 15:41 13 March 2014

For example, different green variations on the map correspond to changes from either corals or seagrasses to other benthic components. These observations are in good agreement with the change detection statistics presented in Tables 2 and 3.

This pattern of change is evident, for example, for the zoomed Shaab El-Erg zone. However, the two light yellow colours dominant in that zone represent sand intertidal areas that changed to areas dominated by macro-algae and coral, respectively, which is also evident from the supervised classification results shown in Figure 6.

Tables 2 and 3 show the initial status classes in columns and the final status classes in rows. Such a layout is required for a complete view of the distribution of pixels that changed classes during the two time periods (1987–2000 and 2000–2013). For each initial state class (i.e. each column), Tables 2 and 3 indicate how these pixels were classified in the final status image. For example, the 10,771 pixels (5.85%) initially classified as coral in 1987 changed to the macro-algae class in 2000, whereas the same change occurred to the 3913 pixels (3.58%) in the 2013 image. The class total row indicates the total number of pixels in each initial status class, while the class total column indicates the total number of pixels in each final status. For instance, Table 2 shows that 184,302 pixels were classified as coral in the 1987 image, while 111,063 pixels were classified as coral in the 2000 image; and Table 3 shows that this coral class ended up with 59,629 pixels in 2013. The class changes row indicates the total number of initial status-assigned pixels that changed to classes other than the original. In other words, ~59% of pixels that were initially classified as coral in 1987 had changed to final status classes other than coral, the equivalent class, but ~67% of the pixels initially classified as coral in 2000 changed to final status classes other than coral. Hence, the class changes row represents the percentage of this specific class that was modified into other classes. The image difference row is

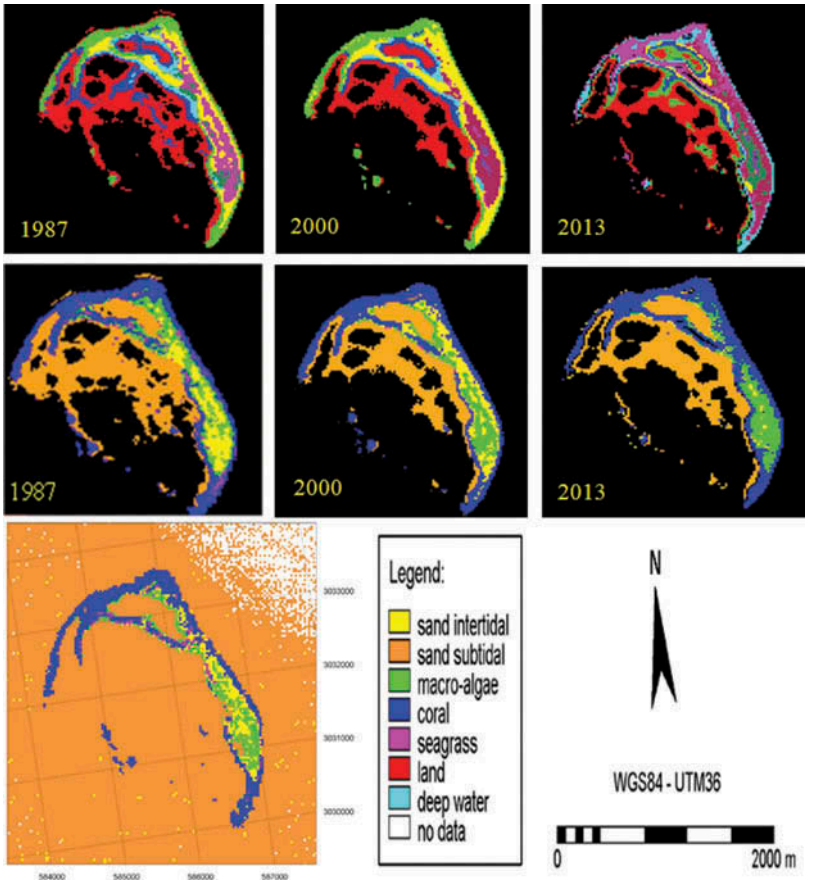


Figure 6. Unsupervised classification results for 1987, 2000, and 2013 (first row, colour bar same as Figure 4) and supervised classification results for 1987, 2000, and 2013 (second row, colour bar same as Figure 5) in Shaab El-Erg area compared to supervised classification results obtained from the literature (Vanderstraete, Goossens, and Ghabour 2004) for the same area in 2000 (third row, colour bar shown here).

simply the difference in the total number of equivalently classed pixels in the two images, computed by subtracting the initial status class totals from the final status class totals. An image difference that is positive indicates that the class size increased. As such, we observe a significant increase in seagrass class of ~93% while the sand intertidal, sand subtidal, and coral expanses show major decreases of ~41%, 37%, and 40%, respectively, between 1987 and 2000. On other hand, we observe a lower increase in the macro-algae class of ~20% while sand intertidal and corals show more drastic declines of ~49% and 45%, respectively, between 2000 and 2013. Sand subtidal and seagrass classes showed a switch in behaviour between the two time periods that may be due to the wide variability in the macro-algae class increase; this will require further investigation, which is beyond the scope of this research. However, this can be attributed to the complexity and unknown magnitude of the phase shift from corals to macro-algae or any other phase shift mechanisms (McManus and Polsenberg 2004; Norström et al. 2009). Bruno et al. (2009) observed a decline in phase shift severity over the Caribbean between 1996 and 2006 but no change in the Florida Keys and Indo-Pacific, deducing thereby that corals

Downloaded by [41.196.240.116] at 15:41 13 March 2014

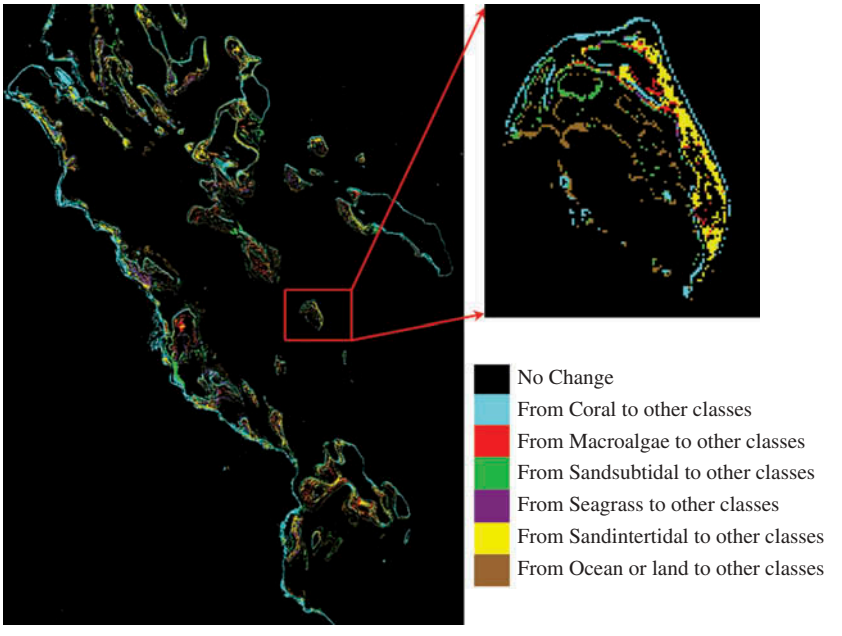


Figure 7. Thematic change detection map for 2000 and 2013 supervised classification coral images. Zoomed image shows changes in benthic composition in the Shaab El-Erg area.

Downloaded by [41.196.240.116] at 15:41 13 March 2014

appear to become more resistant to macro-algal blooms than previously assumed. It is noteworthy that the above-mentioned period overlaps with our second period, 2000–2013. However, there is a lack of knowledge regarding the effects of herbivory on benthic communities in the Red Sea (Jessen and Wild 2013). Burdett et al. (2013) attempted to study the impact of ocean acidification on coastal areas through understanding natural variability. They found that the production of dimethylsulphoniopropionate (DMSP) by marine algae and release of the DMSP breakdown product, dimethylsulphide (DMS), are often related to environmental stress, and applied this to a Red Sea reef system in Egypt. Furthermore, water column DMS/DMSP concentrations were highest over areas dominated by seagrass and macro-algae (dissolved DMS/DMSP) and phytoplankton (particulate DMS/DMSP) rather than corals. Hence our results showing a marked drop in macro-algae increase (~93% to ~20%), in conjunction with the switching of seagrass change (from increasing by ~47% between 1987 and 2000 to decreasing by ~74% between 2000 and 2013), are a key indicator of the above-mentioned stress and match very well with the findings of Burdett et al. (2013).

A general global decline in coral abundance has been observed and attributed to many ecological and man-made factors (Aronson and Precht 2001; Glynn 1993; McManus, Reyes, and Nañola 1997). Coral death due to bleaching or infestation by crown-of-thorns starfish, followed by algal invasion, has been attributed to a number of possible ecological stresses.

(1) The high abundance of macro-algae in inshore reefs compared with offshore reefs has been suggested to be a symptom of the recent widespread decline in those reefs. This decline is apparently attributed to anthropogenic activities and increased sedimentation from the land (Diaz-Pulido and McCook 2008). These

Downloaded by [41.196.240.116] at 15:41 13 March 2014

Table 2. Change detection statistics for coral ecosystem between 1987 and 2000 scenes using supervised classification.

	Scene 1987					
Scene 2000	Coral	Sand subtidal	Sand intertidal	Macro-algae	Seagrass	Class total (Final status
Coral	75167 (40.78%)	3731 (1.99%)	9473 (10.60%)	9666 (23.51%)	4264 (56.74%)	111063 (100%)
Sand subtidal	21894 (11.88%)	76786 (40.89%)	926 (1.04%)	4111 (9.99%)	96 (1.28%)	118030 (100%)
Sand intertidal	16968 (9.21%)	869 (0.46%)	21661 (24.24%)	11027 (26.82%)	1100 (14.64%)	52492 (100%)
Macro-algae	10771 (5.85%)	1463 (0.78%)	52402 (58.63%)	12942 (31.47%)	967 (12.87%)	79269 (100%)
Seagrass	6038 (3.28%)	2688 (1.43%)	652 (0.73%)	1298 (3.16%)	119 (1.58%)	11063 (100%)
Unclassified	53464 (29.01%)	102254 (54.45%)	4257 (4.76%)	2079 (5.06%)	969 (12.89%)	4724718 (100%)
Class total (initial status)	184302 (100%)	187791 (100%)	89371 (100%)	41123 (100%)	7515 (100%)	
Class changes	109135 (59.21%)	111005 (59.11%)	67710 (75.76%)	28181 (68.52%)	7396 (98.41%)	
Image difference	−39.73%	−37.14%	−41.26%	92.76%	47.21%	

Downloaded by [41.196.240.116] at 15:41 13 March 2014

Table 3. Change detection statistics for coral ecosystem between 2000 and 2013 scenes using supervised classification.

	Scene 2000					
Scene 2013	Coral	Sand subtidal	Sand intertidal	Macro-algae	Seagrass	Class total (Final status)
Coral	36144 (33.02%)	1953 (1.38%)	9469 (22.20%)	5232 (7.10%)	2323 (24.00%)	59629 (100%)
Sand subtidal	15466 (14.13%)	96731 (84.96%)	2495 (4.13%)	2776 (3.77%)	5839 (46.02%)	161061 (100%)
Sand intertidal	8016 (7.32%)	401 (0.28%)	17060 (28.27%)	3277 (4.45%)	21 (0.22%)	30908 (100%)
Macro-algae	3913 (3.58%)	1593 (1.12%)	15664 (32.46%)	66333 (82.44%)	1989 (20.55%)	87828 (100%)
Seagrass	403 (0.37%)	570 (0.40%)	325 (0.54%)	656 (0.89%)	558 (5.77%)	2513 (100%)
Unclassified	47121 (41.58%)	16782 (11.85%)	7479 (12.39%)	995 (1.35%)	333 (3.44%)	4253461 (100%)
Class total (initial status)	111063 (100%)	118030 (100%)	52492 (100%)	79269 (100%)	11063 (100%)	
Class changes	73302 (66.98%)	21299 (15.04%)	43288 (71.73%)	12936 (17.56%)	9119 (94.23%)	
Image difference	−45.52%	13.75%	−48.78%	19.22%	−74.03%	



Figure 8. Comparison of urban areas in Hurghada between images from 1987, 2000, and 2013.

activities include urbanization and coastal development, industries including power and desalination plants and refineries, recreation and tourism, waste disposal, waste water treatment facilities, coastal mining and quarrying activities, oil bunkering, and habitat modification, as shown in Figure 8.

(2) Through the Gulf of Suez, a high volume of commercial shipping and heavy tanker traffic passes to the Red Sea. This in turns increases the number of oil spills and major ship groundings on Egyptian coral reefs. Frequent oil spills, together with the phosphate dust that reaches the sea, seem to be among the factors that cause eutrophication in the shallow lagoon waters of the coral region, and consequently the development of algae on coral coasts is stimulated.
(3) Sewage and nutrient loading from hotels and resorts, servicing large numbers of tourists, has directly degraded reefs in the form of fin and anchor damage and boat groundings.
(4) Overfishing also removes important herbivores that graze on algal patches, thus facilitating algal growth and spread.
(5) Climate change may be leading to an overall increase in the total amount of macro-algae and the submergence of some land as a result of rising sea levels (Diaz-Pulido and McCook 2008).

Overgrown algae out-compete coral species for space on the substrate, turning coral reefs into algal reefs. Today, destructive fishing is carried out by the use of home-made explosives composed of fertilizer, fuel, and fuse caps inserted into empty beer bottles (Pilcher and Abou Zaid 2000). Figure 8 shows the development of urban areas over more than two decades in Hurghada, where new recreational villages have encouraged continuous urban extension near coastal areas and even into the open sea. Careless investors build and install huge recreational centres and artificial beaches for the tourism industry without any consideration for ecosystems or resources, thus destroying coral gardens through dredging, sedimentation, extensive landfill operations, and changes to the nature of the reef environment.

Downloaded by [41.196.240.116] at 15:41 13 March 2014

6. Conclusions

Coral reefs at Hurghada have undergone significant decline. They are damaged, displaced, polluted, stepped on, and blasted off, in addition to the effects of climate change on the reefs. One of the most pressing issues affecting reef health is mass coral bleaching that results from an interaction between human activities and climatic changes (Done 1992; McManus and Polsenberg 2004). Data that can be extracted from satellite images improve the ability to identify and assess coral health in a cost- and time-effective manner. This work has demonstrated a new approach that builds on previous studies to applying classification to images without the need to carry out field trips and ground truth measurements. Ground truthing from previous work proved very useful in supporting our training areas that were selected for supervised classification and hence for identification of classes. Unsupervised classification is useful for generating a basic set of classes, and then supervised classification can be used for further definition of these classes. Change detection techniques highlight the differences between the 1987, 2000, and 2013 scenes in a qualitative and quantitative way by subtracting the original and classified images. Thematic difference maps, combined with change detection statistics, tabulate these differences to identify not only where changes have occurred but also the class into which the pixels changed and the levels of these changes. We observed variation in behaviour of class change over the two decades, due potentially to varying stress conditions. During the period 1987–2000, a significant increase in the macro-algae and seagrass classes, accompanied by a major decline in sand intertidal, coral, and sand subtidal classes, was observed. However, during the period 2000–2013, we observed an increase in the sand subtidal and macro-algae classes at the expense of sand intertidal, coral, and seagrass classes.

Downloaded by [41.196.240.116] at 15:41 13 March 2014

Acknowledgements

The authors would like to thank Mr Hany El-Shaer for his generous support in providing some of the satellite images used in our study. Our appreciation is further extended to the editor, Prof. Michael Collins, co-editor-in-chief Prof. Arthur Cracknell, and the anonymous reviewers for their helpful comments that enhanced this paper. Furthermore, the authors would like also to acknowledge the use of the Samueli Laboratory in Computational Sciences in the Schmid College of Science and Technology, Chapman University, for image processing and data analysis.

References

Ahmad, W., and D. T. Neil. 1994. “An Evaluation of Landsat Thematic Mapper (TM) Digital Data for Discriminating Coral Reef Zonation: Heron Reef (GBR).” *International Journal of Remote Sensing* 15 (13): 2583–2597. doi:10.1080/01431169408954268.

Armstrong, R. A. 1993. “Remote Sensing of Submerged Vegetation Canopies for Biomass Estimation.” *International Journal of Remote Sensing* 14: 621–627. doi:10.1080/01431169308904363.

Aronson, R. B., and W. F. Precht. 2001. “White-Band Disease and the Changing Face of Caribbean Coral Reefs.” *Hydrobiologia* 460: 25–38. doi: 10.1023/A:1013103928980.

Atkinson, M. J., P. G. Lucey, G. J. Taylor, J. Porter, S. Dollar, and S. Andre. 2001. CRESPO: *Coral Reef Ecosystem Spectro-Photometric Observatory, Concept Study Report to the University Earth System Science Program, National Aeronautics and Space Administration*. Honolulu: University of Hawaii.

Biña, R. T., C. Carpenter, W. Zacher, R. S. Jara, and J. B. Lim. 1978. “Coral Reef Mapping Using Landsat Data: Follow up Studies.” *Proceedings of the 12th International Symposium on Remote Sensing of Environment* 1: 2051–2070.

Bruno, J. F., H. Sweatman, W. F. Precht, E. R. Selig, and V. G. W. Schutte. 2009. "Assessing Evidence of Phase Shifts from Coral to Macroalgal Dominance on Coral Reefs." *Ecology* 90: 1478–1484. doi: 10.1890/08-1781.1.

Burdett, H. L., P. J. C. Donohue, A. D. Hatton, M. A. Alwany, and N. A. Kamenos. 2013. "Spatiotemporal Variability of Dimethylsulphoniopropionate on a Fringing Coral Reef: The Role of Reefal Carbonate Chemistry and Environmental Variability." *PLoS ONE* 8 (5): e64651–. doi: 10.1371/journal.pone.0064651.

Diaz-Pulido, G., and L. McCook. 2008. "Macroalgae (Seaweeds)." In *The State of the Great Barrier Reef On-Line*, edited by C. A. Townsville, 1–44. Townsville: Great Barrier Reef Marine Park Authority.

Done, T. J. 1992. "Phase Shifts in Coral Reef Communities and Their Ecological Significance." *Hydrobiologia* 247: 121–132. doi: 10.1007/BF00008211.

Edwards, A., ed. 1999. *Applications of Satellite and Airborne Image Data to Coastal Management*. Paris: UNESCO.

Edwards, F. J. 1987. "Climate and Oceanography." In *Key Environments: Red Sea*, edited by A. J. Edwards and S. M. Head, 45–69. Oxford: Pergamon Press.

El-Raey, M., A. Abdel Kader, S. Nasr, and H. El Gamily. 1996. "Remote Sensing and GIS for an Oil Spill Contingency Plan, Ras-Mohammed, Egypt." *International Journal of Remote Sensing* 17 (11): 2013–2026. doi: 10.1080/01431169608948756.

Glynn, P. W. 1993. "Coral Reef Bleaching: Ecological Perspectives." *Coral Reefs* 12: 1–17. doi: 10.1007/BF00303779.

Green, E. P., P. J. Mumby, A. J. Edwards, and C. D. Clark. 2000. *Remote Sensing Handbook for Tropical Coastal Management*, edited by A. J. Edwards. Paris: UNESCO.

Hochberg, E. J., and M. J. Atkinson. 2003. "Capabilities of Remote Sensors to Classify Coral, Algae, and Sand as Pure and Mixed Spectra." *Remote Sensing of Environment* 85 (2): 174–189. doi: 10.1016/S0034-4257(02)00202-X.

Jessen, C., and C. Wild. 2013. "Herbivory Effects on Benthic Algal Composition and Growth on a Coral Reef Flat in the Egyptian Red Sea." *Marine Ecology Progress Series* 476: 9–21. doi: 10.3354/meps10157.

Kutser, T., A. G. Dekker, and W. Skirving. 2003. "Modeling Spectral Discrimination of Great Barrier Reef Benthic Communities by Remote Sensing Instruments." *Limnology and Oceanography* 48 (1): 497–510. doi: 10.4319/lo.2003.48.1_part_2.0497.

Lillesand, T. M., and R. W. Kiefer. 2000. *Remote Sensing and Image Interpretation*. 4th ed. New York: Wiley.

Lyzenga, D. 1978. "Passive Remote Sensing Techniques for Mapping Water Depth and Bottom Features." *Applied Optics* 17 (3): 379–383. doi:10.1364/AO.17.000379.

Lyzenga, D. 1981. "Remote Sensing of Bottom Reflectance and Water Attenuation Parameters in Shallow Water Using Aircraft and Landsat Data." *International Journal of Remote Sensing* 2 (1): 71–82. doi: 10.1080/01431168108948342.

Maritorena, S. 1996. "Remote Sensing of the Water Attenuation in Coral Reefs: A Case Study in French Polynesia." *International Journal of Remote Sensing* 17 (1): 155–166. doi: 10.1080/01431169608948992.

Matsunaga, T., A. Hoyano, and Y. Mizukami. 2001. "Monitoring of Coral Reefs on Ishigaki Island in Japan Using Multitemporal Remote Sensing Data." *Hyperspectral Remote Sensing of the Ocean* 4154: 212–222. doi: 10.1117/12.411677.

McManus, J. W., and J. F. Polsenberg. 2004. "Coral–Algal Phase Shifts on Coral Reefs: Ecological and Environmental Aspects." *Progress in Oceanography* 60: 263–279. doi: 10.1016/j.pocean.2004.02.014.

McManus, J. W., R. B. Reyes, Jr., and C. L. Nañola, Jr. 1997. "Effects of Some Destructive Fishing Methods on Coral Cover and Potential Rates of Recovery." *Environmental Management* 21: 69–78. doi:10.1007/s002679900006.

Moufaddal, W. M. 2005. "Use of Satellite Imagery as Environmental Impact Assessment Tool: A Case Study from the NW Egyptian Red Sea Coastal Zone." *Environmental Monitoring and Assessment* 107: 427–452. doi: 10.1007/s10661-005-3576-2.

Mumby, P. J., E. P. Green, A. J. Edwards, and C. D. Clark. 1997. "Coral Reef Habitat-Mapping: How Much Detail can Remote Sensing Provide?" *Marine Biology* 130 (2): 193–202. doi: 10.1007/s002270050238.

Downloaded by [41.196.240.116] at 15:41 13 March 2014

Mumby, P. J., W. Skirving, A. E. Strong, J. T. Hardy, E. F. LeDrew, E. J. Hochberg, R. P. Stumpf, and L. T. David. 2004. "Remote Sensing of Coral Reefs and their Physical Environment." *Marine Pollution Bulletin* 48 (3–4): 219–228.

Norström, A. V., M. Nyström, J. Lokrantz, and C. Folke. 2009. "Alternative States on Coral Reefs: Beyond Coral–Macroalgal Phase Shifts." *Marine Ecology Progress Series* 376: 295–306. doi: 10.3354/meps07815.

PCRF (Planetary Coral Reef Foundation Overview organization). 2002. "Mapping Coral Reefs From Space." Accessed May 15, 2013. http://www.pcrf.org/.

PERSGA. 2004. "The Regional Organization for the Conservation of the Environment of the Red Sea and Gulf of Aden." Accessed May 15, 2013. http://www.persga.org.

Pilcher, N., and M. Abou Zaid. 2000. "The Status of Coral Reefs in Egypt." In *Status of Coral Reefs of the World: 2000*, edited by C. Wilkinson, 1–17. Townsville: Australian Institute of Marine Science.

Pilcher, N., and A. Alsuhaibany. 2000. "Regional Status of Coral Reefs in the Red Sea and the Gulf of Aden." In *Status of Coral Reefs in The World: 2000*, edited by C. Wilkinson, 35–54. Townsville: AIMS.

Purkis, S. J., and R. Pasterkamp. 2004. "Integrating in Situ Reef-Top Reflectance Spectra with Landsat TM Imagery to Aid Shallow-Tropical Benthic Habitat Mapping." *Coral Reefs* 23 (1): 5–20. doi: 10.1007/s00338-003-0351-0.

Smith, V. E., R. H. Rogers, and L. H. Reed. 1975. "Thematic Mapping of Coral Reefs Using Landsat Data." *Proceedings of 10th International Symposium on Remote Sensing of Environment* 1: 585–594.

Stoddart, D. R. 1969. "Ecology and Morphology of Recent Coral Reefs." *Biological Reviews of the Cambridge Philosophical Society* 44: 433–498. doi: 10.1111/j.1469-185X.1969.tb00609.x.

Vanderstraete, T., R. Goossens, and T. K. Ghabour. 2004. "Coral Reef Habitat Mapping in The Red Sea (Hurghada, Egypt) Based on Remote Sensing." *EARSeL eProceedings* 3 (2): 191–207.

Vanderstraete, T., R. Goossens, and T. K. Ghabour. 2006. "The Use of Multi-Temporal Landsat Images for the Change Detection of the Coastal Zone Near Hurghada, Egypt." *International Journal of Remote Sensing* 27 (17): 3645–3655. doi: 10.1080/01431160500500342.

Wilson, M. 1998. "The GEF Egyptian Red Sea Coastal and Marine Resource Management Project – A Decade of Effort, Experience and Trade-Offs Required to Achieve Marine Tourism and Conservation Goals." In *International Tropical Marine Ecosystems Management Symposium Proceedings*, 239–250. Townsville: GBRMPA.

Wilkinson, C., ed. 2000. *Status of Coral Reefs of The World: 2000*. Townsville: Australian Institute of Marine Science.

Downloaded by [41.196.240.116] at 15:41 13 March 2014

View publication stats